



Full paper/Mémoire

Antibacterial inactivation of spiramycin after titanium dioxide photocatalytic treatment



Rahma Hendili ^{a, b}, Abir Alatrache ^a, Mossadok Ben-Attia ^b,
Marie-Noëlle Pons ^{c, *}

^a Laboratoire de RMN-Physique, École nationale supérieure des ingénieurs de Tunis, Université de Tunis, 5, avenue Taha-Hussein, BP 56, Bab Menara 1008, Tunis, Tunisia

^b Laboratoire de biosurveillance de l'Environnement (LR01/ES14), Faculté des sciences de Bizerte, Université de Carthage, route de Tunis, Zarzouna 7021, Tunisia

^c Laboratoire Réactions et Génie des procédés – UMR CNRS 7274, Université de Lorraine, ENSIC, 1, rue Grandville, BP 20451, 54001 Nancy cedex, France

ARTICLE INFO

Article history:

Received 4 November 2016

Accepted 23 February 2017

Available online 30 March 2017

Keywords:

Antibacterial activity

AOP

Macrolide

Spiramycin

TiO₂ immobilization

ABSTRACT

The photocatalytic degradation of an antibiotic (spiramycin) has been studied using immobilized titanium dioxide (TiO₂) as a photocatalyst in a laboratory reactor under ultraviolet illumination (365 nm). The degradation of the antibiotic was monitored by ultraviolet spectrophotometry and high-pressure liquid chromatography and confirmed by an antibacterial activity evaluation. Two types of TiO₂ (P25 and PC500) immobilized on glass plates were compared. For TiO₂ PC500 immobilization on glass and paper was also studied. A slightly better degradation was obtained with TiO₂ P25 for which the degradation kinetics were investigated. The Langmuir–Hinshelwood kinetic model is satisfactorily obeyed at initial time and in the course of the reaction. Adsorption and apparent rate constants were determined. These results show a complete degradation of spiramycin, which was confirmed by the inhibition of the antibacterial activity of *Staphylococcus xylosus*, when exposed to spiramycin solutions treated with photocatalyst for a short time. In addition, the codegradation of spiramycin and tylosin was investigated and showed that tylosin had a higher affinity to the catalyst TiO₂ P25 than spiramycin. The complete degradation of spiramycin confirms the feasibility of such a photocatalytic treatment process for spiramycin elimination from contaminated water.

© 2017 Académie des sciences. Published by Elsevier Masson SAS. This is an open access article under the CC BY-NC-ND license (<http://creativecommons.org/licenses/by-nc-nd/4.0/>).

R É S U M É

La dégradation photocatalytique d'un antibiotique (spiramycine) a été étudiée en utilisant comme photocatalyseur du dioxyde de titane immobilisé dans un réacteur de laboratoire sous illumination UV (365 nm). La dégradation de l'antibiotique a été suivie par spectrophotométrie UV–visible et HPLC et a été confirmée par une évaluation de l'activité antibactérienne. Deux types de TiO₂ (P25 et PC500) immobilisés sur des plaques de verre ont été comparés. Pour le TiO₂ PC500 l'immobilisation sur du verre et du papier a aussi été étudiée. La dégradation a été un peu meilleure pour le TiO₂ P25, pour lequel la cinétique a été étudiée. Le modèle de Langmuir–Hinshelwood est suivi de façon satisfaisante à la fois

Mots clefs:

activité antibactérienne

immobilisation de TiO₂

macrolide

POA

spiramycine

* Corresponding author.

E-mail address: marie-noelle.pons@univ-lorraine.fr (M.-N. Pons).

au début et au cours de l'expérience. Les constantes d'adsorption et de vitesse apparentes ont été déterminées. Ces résultats montrent la dégradation complète de la spiramycine et a été confirmée par l'inhibition de son action sur la croissance de *S. xyloso*. De plus la co-dégradation de la spiramycine et de la tylosine a été étudiée et a montré une plus grande affinité de la tylosine pour le TiO₂ P25, par rapport à la spiramycine. La dégradation complète de la spiramycine confirme la faisabilité d'un traitement photocatalytique pour l'élimination de cet antibiotique d'eaux contaminées.

© 2017 Académie des sciences. Published by Elsevier Masson SAS. This is an open access article under the CC BY-NC-ND license (<http://creativecommons.org/licenses/by-nc-nd/4.0/>).

1. Introduction

Since the 1900s, the modern world is experiencing a period of great expansion particularly in agriculture and industry. The discharge of nontreated or badly treated industrial and urban effluents into rivers, aquifers, and lakes [1] coupled with the intensification of agriculture creates a multicontaminant pollution of the aquatic environment. Because of the emergence of new analytical methods, micropollutants (at concentrations lower than a few micrograms per liter) are detected in the different aquatic compartments [2,3]. The range of these micropollutants is very large: metals, pharmaceuticals, detergents, fire retardants, and so forth. Several kinds of drugs, such as antibiotics, synthetic hormones, analgesics, and so forth, have been identified in surface water, groundwater, sewage water, and drinking water [4]. Some of them are not significantly adsorbed in the subsoil and may leach into groundwater [5]. In addition, they have a direct effect on the environment by disrupting the ecosystem equilibrium [6]. Finally, environmental bacteria exposed to residual antibiotics could modify their genetic information, developing higher antibiotic resistance and resulting in multi-resistant bacterial strains [4]. Antibiotics from the macrolide family, such as spiramycin and tylosin, have been extensively used in human and veterinary medicine to treat and prevent bacterial infections [7].

The high cost of physicochemical treatment processes and the limitation of biological treatment led scientists to develop other methods to offer attractive alternatives such as advanced oxidation processes (AOPs) to cope with these micropollutants, which are largely recalcitrant to biological degradation. Chemical treatment by AOPs results in a nonselective oxidation of most organic compounds up to complete mineralization into CO₂ and other inorganic compounds. AOPs such as ultraviolet (UV)–peroxide combinations, ozonation, or photo-Fenton processes have demonstrated their effectiveness in the oxidation of nonbiodegradable organic compounds. Another AOP, photocatalysis, has gradually become an alternative technology to clean up the water. It has been investigated on some antibiotics [8,9]. The photocatalyst is mainly a semiconductor (oxide or sulfide). The most commonly used semiconductor is titanium dioxide (TiO₂), because of its performance, stability, low cost, and resistance to corrosive conditions. Its gap energy is 3.2 eV. This energy can be supplied by the exposure of this material to a UV irradiation around 365 nm. The benefits of TiO₂ are the use of a stable,

nontoxic, and inexpensive photocatalyst, which can be activated by natural and artificial light sources.

The aim of this work is to study the degradation of spiramycin by photocatalysis to assess the parameters governing the antibiotic degradation kinetics and the efficiency of the photocatalyst deposit. The influence of experimental conditions, such as flow rate, and the presence of another macrolide (tylosin) in the treated solution were also investigated. To confirm the complete transformation of spiramycin, the antibacterial activity was investigated, with the treated solutions inoculated with *Staphylococcus xyloso* strain.

2. Materials and methods

2.1. Antibiotics

Spiramycin (Fig. 1) active ingredient offered by SAIPH Laboratories, Tunisia (Arab Society of Pharmaceutical Industries) was used without any further purification. Spiramycin is a mixture of three types (Spiramycin I up to 85%, Spiramycin II, and Spiramycin III), depending on the group borne by the carbon 3 of the cycle [10]. Tylosin tartrate (Fig. 2) was purchased from Sigma–Aldrich (Saint-Quentin-Fallavier, France) and used without further purification.

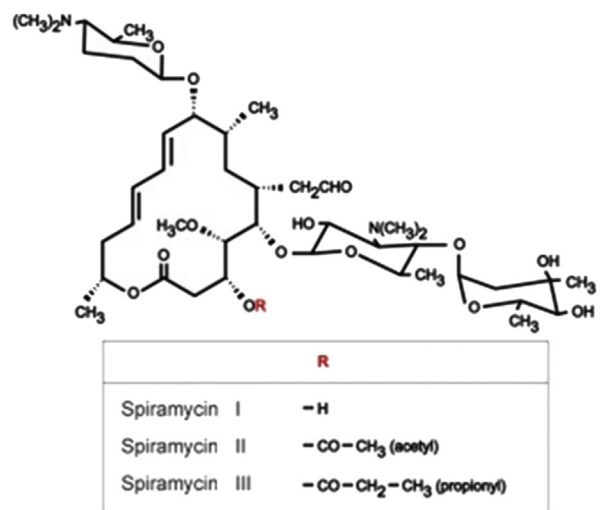


Fig. 1. Spiramycin.

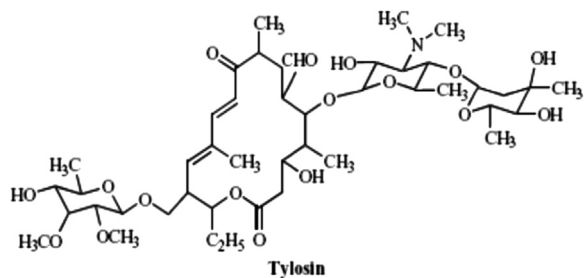


Fig. 2. Tylosin.

2.2. Photocatalysts

Two different TiO_2 powders were tested: P25 from Degussa (Frankfurt, Germany) (80% anatase and 20% rutile), and PC500 from Millennium Inorganic Chemicals (Paris, France) (mainly anatase). The manufacturers' specifications are reported in Table 1.

2.3. Experimental setup and procedures

The experiments were conducted in a reactor (Fig. 3) composed of a parallelepiped tank glass on the bottom of which is placed the immobilized photocatalyst, either a glass slide (surface = 0.019 m^2) or the nonwoven paper. Photocatalyst deposition on HF-pretreated glass slide has been detailed elsewhere [11]. PC500 immobilized on nonwoven paper made of cellulose fibers was kindly provided by Ahlstrom Research (Pont-Evêque, France): the coating is performed by a mixture of TiO_2 and SiO_2 ($\text{TiO}_2/\text{SiO}_2$ mass ratio: 1) using a size press. The combination of cellulose fibers, TiO_2 and SiO_2 , is referred to as the photocatalyst material in this study. The final load of TiO_2 (after washing the paper) is about 18 g/m^2 .

Irradiation was carried out by a Philips 8 W UV fluorescent lamp, emitting at around 365 nm, positioned parallel to the reactor (distance to the photocatalyst = 6.3 cm). The average photon irradiance, as measured by a VLX-3W radiometer (Vilber Lourmat Deutschland GmbH, Eberhardzell, Germany) was 1.25 mW/cm^2 . The recycling of the solution to be treated is ensured by means of a peristaltic pump.

The degradation of spiramycin was monitored by HPLC or UV spectrophotometry and microbiologic assays. Spectrophotometric measurements were carried out on an OPTIMA SP 3000 UV–vis spectrophotometer with a quartz cuvette (path length = 1 cm). The maximum absorbance

Table 1
Manufacturer's specifications of the TiO_2 photocatalyst.

Specification	P25	PC500
Appearance	White powder	White powder
Composition	80% Anatase, 20% rutile	100% Anatase
Elementary particle size (nm)	Approximately 20	10–15
Pore size (Å)	Nonporous	54
Specific surface area ($\text{m}^2 \text{ g}^{-1}$)	50 ± 15	375

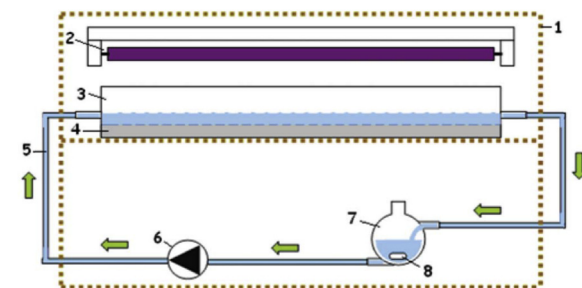


Fig. 3. Experimental setup: (1) cover, (2) fluorescent UV lamp, (3) reactor, (4) immobilized photocatalyst, (5) polytetrafluoroethylene tubing, (6) peristaltic pump, (7) reservoir, and (8) magnetic stirrer.

wavelengths of spiramycin and tylosin were identified at 230 and 290 nm, respectively. HPLC was carried out with a Shimadzu SPD-10A equipped with a spectrophotometric detector, and a Lichrosorb C18 column $250 \times 4.6 \text{ mm}$, using as a mobile phase of mixture of 60% methanol and 40% water at a flow rate of 1 mL min^{-1} . The retention time was about 10 min.

Bioassays were carried according to the modified methodology of San Martin et al. [12]. *S. xylosus* was used as an assay microorganism. After plating the bacterial strain on plates containing a Casein Tryptone-Soy medium and incubation at 37°C for 24 h, a few bacterial colonies were removed and suspended in 5 mL of physiological saline (0.9%) to form a dense bacterial suspension. Mueller–Hinton agar plates were loaded with a $4.10^6 \text{ CFU mL}^{-1}$ suspension of *S. xylosus*. Small wells made in the agar were inoculated with 100 μL of irradiated spiramycin samples. After 24 h of incubation at 37°C , the inhibition halo diameters were measured and reported in millimeters.

3. Results and discussion

3.1. Photocatalytic degradation of spiramycin

The spiramycin absorbance was monitored at different irradiation times, as shown in Fig. 4. The absorbance

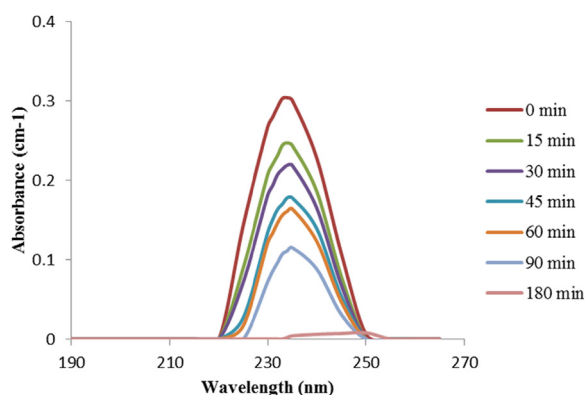


Fig. 4. Variation of spiramycin solution absorbance spectra as a function of the irradiation time on TiO_2 P25.

decreases with time indicating a degradation of spiramycin, and the absence of the eventual formation of light-absorbing byproducts was observed.

3.2. Evidence of photocatalytic activity

Three runs were conducted for this experiment: (1) with UV only (photolysis), (2) with TiO₂ only (adsorption), and (3) with TiO₂ and UV light (photocatalysis) as shown in Fig. 5. For each run, spiramycin solution was first recycled in the photocatalytic reactor in the dark for 60 min, to allow the establishment of the adsorption equilibrium. This equilibrium is reached after 30 min.

No degradation was observed under irradiation in the absence of a catalyst, which is in agreement with the fact that the UV lamp emits at $\lambda = 365$ nm, whereas the molecule absorbs at $\lambda = 234$ nm (Fig. 4). The adsorption equilibrium was reached after 30 min [13]. Once the UV lamp is turned on, the photocatalytic reaction starts and the absorbance is decreasing with time, indicating the degradation of the spiramycin molecule.

When TiO₂ is irradiated with photons whose energy is equal to or greater than its band gap energy ($E_G = 3.2$ eV), that is, supplied by light at $\lambda = 365$ nm, electron–hole pairs are created. In an aqueous system, holes react with H₂O or OH⁻ adsorbed at the surface of the semiconductor to produce OH[•] radicals, which are the most oxidizing species in this process. On the other hand, electrons are trapped at surface sites and removed by reactions with adsorbed molecular O₂ to form superoxide anion radical O₂^{-•} (or H₂O^{•+}) [14].

3.3. Effect of the initial concentration and order of the photocatalytic reaction

The photocatalytic degradation of spiramycin was conducted with different initial concentrations ranging from 5 to 25 mg L⁻¹ with both different TiO₂ types (P25 immobilized on glass slides and PC500 immobilized either on glass slides or on nonwoven paper), with a recycle flow rate of 0.4 L min⁻¹ (Fig. 6).

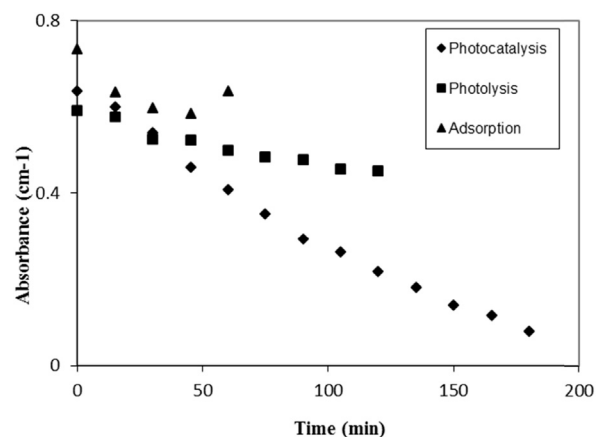


Fig. 5. Fate of spiramycin (initial concentration = 25 mg L⁻¹) by photolysis, adsorption, and photocatalysis (catalyst, TiO₂ P25).

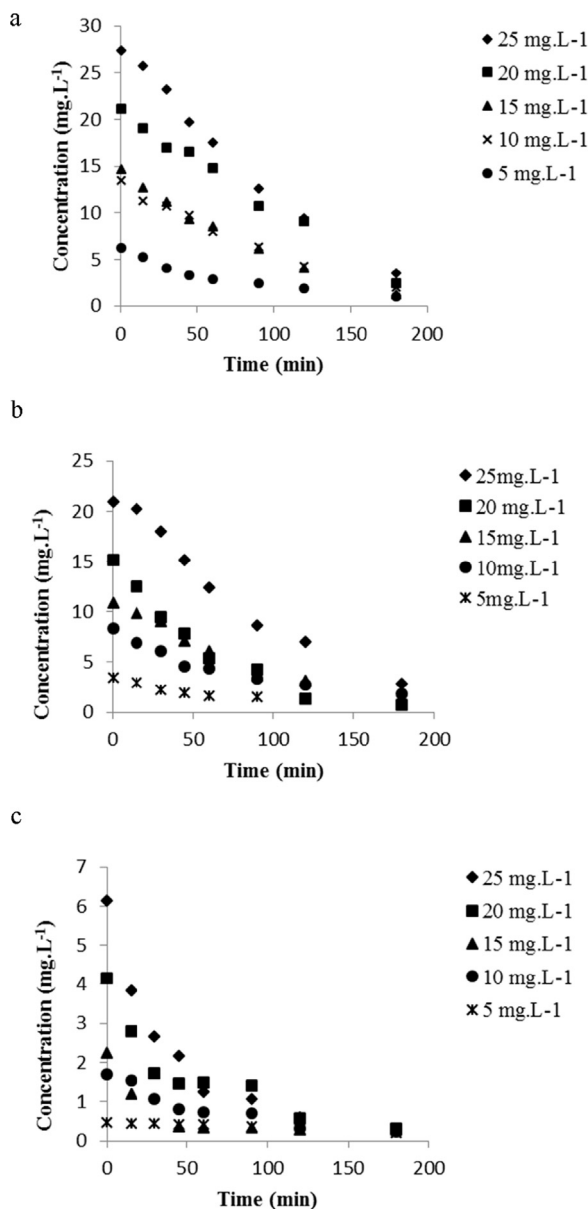


Fig. 6. Effect of the initial concentrations of spiramycin on the photocatalytic degradation: (a) TiO₂ P25; (b) TiO₂ PC500 on glass slide; and (c) TiO₂ PC500 on nonwoven paper.

The kinetics of degradation increases as the initial concentration decreases. This phenomenon observed in the case of tylosin [15] and both in liquid phase [16] and in the gas phase [17] with other substances can be interpreted by the saturation of the surface of TiO₂ with high concentrations of spiramycin. Spiramycin appears to be completely degraded after 180 min whatever the initial concentration. The absorbance spectra decreased with time in these experimental conditions indicating that no light-absorbing byproducts were formed. This could be explained by the fact that spiramycin, which is an organic molecule, has been degraded because of the photoexcitation of the semiconductor (TiO₂ P25 or PC500) [18], giving rise to

highly reactive hydroxyl radicals that ensure complete mineralization of spiramycin [19,20].

Similar results were obtained for both types of catalysts (Fig. 6), but with a higher adsorption onto TiO₂ P25. This indicates that TiO₂ P25 has more active sites providing the adsorption of the molecule, which has been previously observed [21]. However, an important relative adsorption was obtained with the nonwoven paper, which is because of the much higher loading of a photocatalyst on this support (18 against 1.8 g/m² for the glass slides prepared in the laboratory).

In the Langmuir–Hinshelwood (LH) model, the rate of reaction is proportional to the surface coverage by the pollutant. Assuming such a model of adsorption, the rate of reaction is given by the relationship [22,23]

$$r_0 = k_{\text{deg}} \frac{K_{\text{LH}} C_0}{1 + K_{\text{LH}} C_0} \quad (1)$$

where K_{LH} is the adsorption constant, C_0 is the spiramycin concentration in the aqueous phase, and k_{deg} is a kinetic constant, which depends on the irradiation conditions. Eq. 1 can be rewritten in a linear form as

$$\frac{C_0}{r_0} = \left(\frac{1}{k_{\text{deg}}} \right) \left(\frac{1}{K_{\text{LH}}} + C_0 \right) \quad (2)$$

From the plot of C_0/r_0 against the initial concentration C_0 , the data were consistent with this linear relationship. From the slope and intercept of the obtained straight line, the constants K_{LH} and k_{deg} were determined (0.013, 0.86) for P25, (0.095, 0.21) for PC500, and (0.015 L mg⁻¹, 0.42 mg L⁻¹ min⁻¹) for Ahlstrom paper, respectively. Then, theoretical curves have been plotted in Figs. 7–9 and agree with the experimental data. As a consequence, the order of the reaction with respect to spiramycin is close to 1 at low concentration (i.e., $C_0 < 25$ mg L⁻¹), when Eq. 1 reduces to Eq. 3:

$$r_0 = k_{\text{deg}} K_{\text{LH}} C_0 \quad (3)$$

whereas the order tends to 0 at high concentrations.

A satisfactory fitting is observed regarding the rate variation with the initial concentration of spiramycin. The

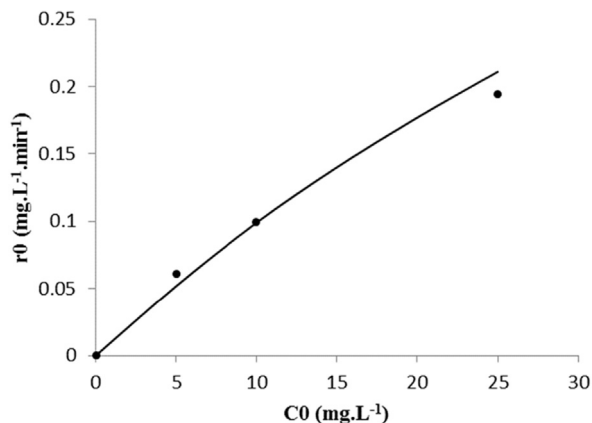


Fig. 7. Kinetic model for spiramycin degradation on TiO₂ P25 catalyst. (●) Experimental data and (–) model.

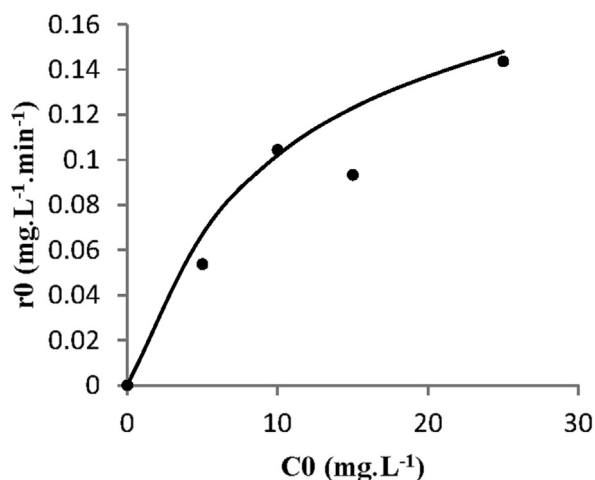


Fig. 8. Kinetic model for spiramycin degradation on TiO₂ PC500 catalyst. (●) Experimental data and (–) model.

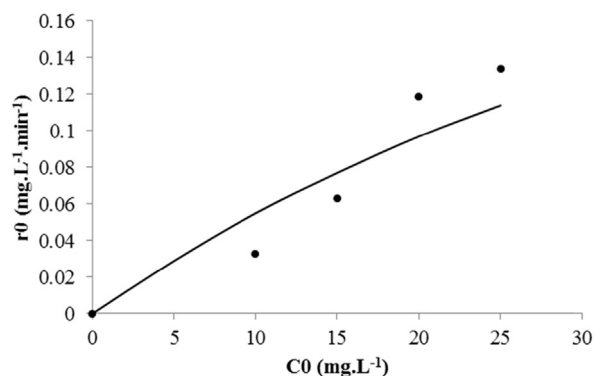


Fig. 9. Kinetic model for spiramycin degradation on TiO₂ PC500 immobilized on nonwoven paper. (●) Experimental data and (–) model.

standard deviation was 0.022 mg L⁻¹ min⁻¹ for PC500 on glass slides, 0.013 mg L⁻¹ min⁻¹ for the PC500 on nonwoven paper, and 0.011 mg L⁻¹ min⁻¹ for P25 on glass slides. Therefore, it was concluded that the photocatalysis of spiramycin obeys a simple LH kinetic model.

3.4. Effect of flow rate

In heterogeneous photocatalysis the reaction kinetics are determined by mass transfer, chemical reaction, and chemisorption [22]. Mass transfer is so fast that there is no diffusion limitation, and thus chemical kinetics determine the observed rate.

Experiments were conducted by varying the solution flow circulation. The values of the flow rate range from 152 to 428 mL min⁻¹, for a concentration of 25 mg L⁻¹ of spiramycin, using PC500 immobilized on nonwoven paper. As shown in Fig. 10, the rate r_0 is nearly independent of the flow rate (variation of 10%); thus the flow rate has no effect on the rate of photocatalytic degradation, which indicates the absence of the external mass-transfer limitation. Such

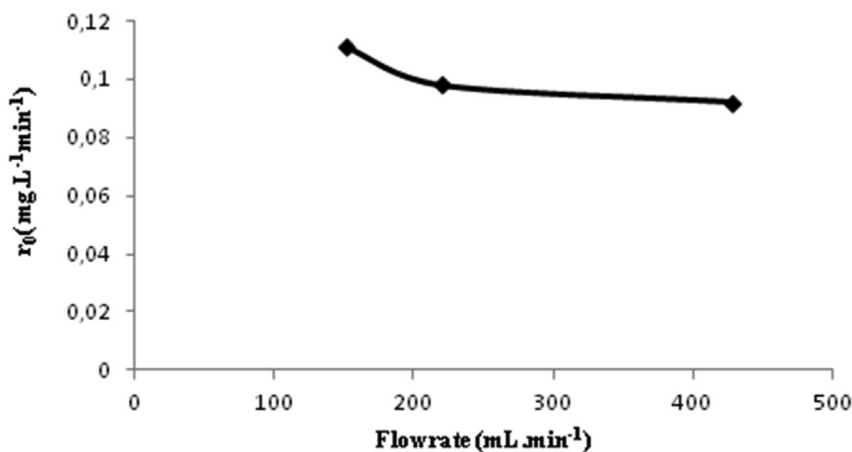


Fig. 10. Influence of the flow rate on the initial rate of photocatalytic degradation of spiramycin (r_0) for TiO₂ PC500 immobilized on nonwoven paper.

observation has already been made for an earlier study [24].

3.5. TiO₂ photocatalysis effect on the antibacterial activity

To assess the antibacterial activity of spiramycin during photocatalysis, experiments were conducted on agar plates inoculated with a pathogenic bacteria strain belonging to the species *S. xylosus* isolated from sediments of the Bizerte lagoon near the treatment plant Sidi Hmed [25]. Typical results appear in Fig. 11, where a significant reduction in the diameters of zones of inhibition halo was observed after 45 min of contact of spiramycin solutions with the catalyst. After 2 h of photocatalytic treatment, a total loss of antibacterial activity was observed. This demonstrates that the treated spiramycin does not present antibacterial properties anymore. These results show a modification in the molecule structure by the photocatalytic process as it has

been shown by Palominos et al. [9] in their work on photocatalytic degradation of another antibiotic (oxolinic acid). Other researchers [26–28] have described the inhibition of the pollutant activity after photocatalysis, in their respective investigations.

3.6. Codegradation

Discharges of domestic and industrial wastewater can be polluted by several organic compounds in varying concentrations. The simultaneous existence of a variety of pollutants may affect the treatment process, because it depends on the accessibility of the surface sites of the catalyst, in addition to competitive degradation that may occur among the pollutants. To study this phenomenon, the degradation of a binary mixture of spiramycin and tylosin as copollutants was conducted using concentrations of 20 and 30 mg L⁻¹, respectively, on TiO₂ PC500 and P25

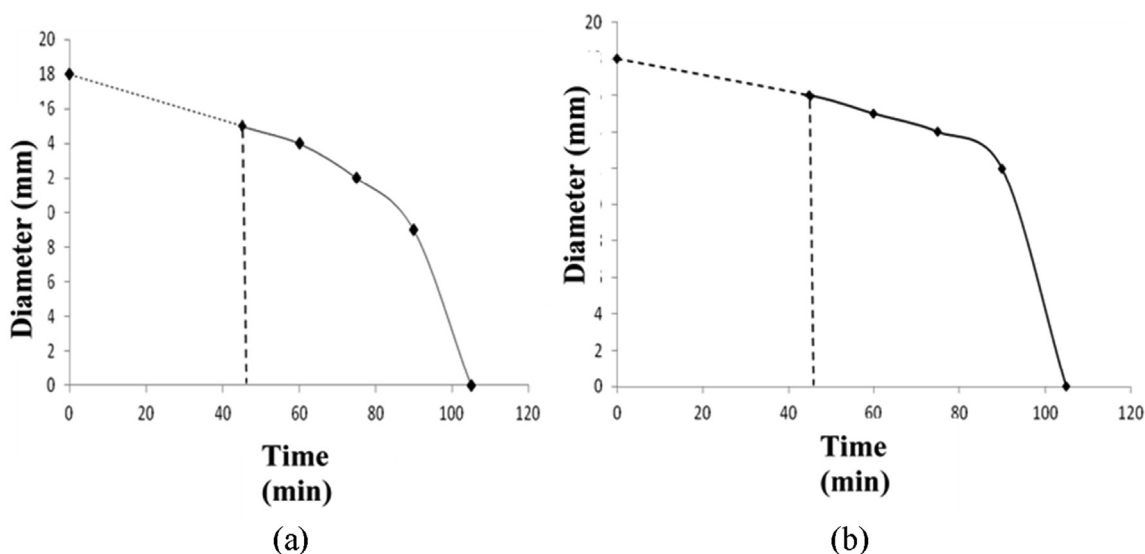


Fig. 11. Antibacterial activity evolution of the spiramycin solution. TiO₂ (----), TiO₂ + UV (—), (a) on TiO₂ P25; (b) on TiO₂ PC500.

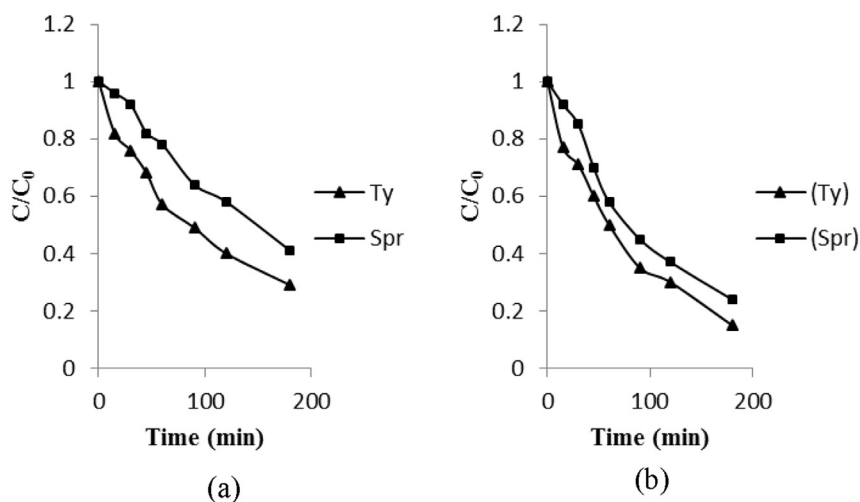


Fig. 12. Codegradation of spiramycin and tylosin on (a) TiO_2 P25 and (b) TiO_2 PC500. Initial concentrations: [Spr] = 20 mg L⁻¹; [Ty] = 30 mg L⁻¹.

immobilized on glass slides. The experimental results are plotted in Fig. 12(a) for TiO_2 P25 and Fig. 12(b) for TiO_2 PC500.

It appears that TiO_2 P25 is more efficient than TiO_2 PC500 for degradation of both antibiotics. In addition, tylosin has a higher relative affinity to the catalyst than spiramycin. The degradation of these two antibiotics occurs simultaneously without mutual inhibition; in this case, it seems that there is no competitive adsorption on the surface of each of the two catalysts. A similar behavior has been reported in the codegradation of isoproturon–phenol codegradation [29].

4. Conclusions

This study highlighted the effectiveness of photocatalysis using immobilized TiO_2 on the degradation of spiramycin. The type of the used catalyst is not significant in the photocatalytic process. The effect of spiramycin initial concentrations was investigated and showed that the kinetic obeys to LH kinetics model. Thus, adsorption constants and apparent kinetic rate constants have been determined and no external mass transfer limitation has been observed. The study of the antibacterial activity of this molecule was performed and allowed demonstrating that this activity was completely inhibited after photocatalysis treatment, confirming the chemical analysis. The codegradation of spiramycin and tylosin showed the absence of competitive adsorption of these two antibiotics on the surface of a catalyst and thus a simultaneous degradation could occur.

References

- [1] D. Barcelo, M. Petrovic, *TrAC, Trends Anal. Chem.* 26 (2007) 1019.
- [2] T. Heberer, *Toxicol. Lett.* 131 (2002) 5.
- [3] S.D. Costanzo, J. Murby, J. Bates, *Mar. Pollut. Bull.* 51 (2005) 218.
- [4] M. Petrovic, S. Gonzalez, D. Barcelo, *TrAC, Trends Anal. Chem.* 22 (2003) 685.
- [5] P. Calza, S. Marchisio, C. Medana, C. Baiocchi, *Anal. Bioanal. Chem.* 396 (2010) 1539.
- [6] C. Tixier, H.P. Singer, S. Oellers, S.R. Muller, *Environ. Sci. Technol.* 37 (2003) 1061.
- [7] E. Abu-Gharbieh, V. Vasina, E. Poluzzi, F. DePonti, *Pharmacol. Res.* 50 (2004) 211.
- [8] C. Reyes, J. Fernandez, J. Freer, M.A. Mondaca, C. Zaror, S. Malato, H.D. Mansilla, *J. Photochem. Photobiol., A* 184 (2006) 141.
- [9] R.A. Palominos, A. Mora, M.A. Mondaca, M. Perez-Moya, H.D. Mansilla, *J. Hazard. Mater.* 158 (2008) 460.
- [10] S. Kernbaum, *Sem. Hop. Paris* 58 (1982) 289.
- [11] C. Hachem, F. Bocquillon, O. Zahraa, M. Bouchy, *Dyes Pigm.* 49 (2001) 117.
- [12] B. San Martin, H. Canon, A. Quiroz, P. Hernandez, *Av. Cienc. Vet.* 15 (2000) 37.
- [13] M.G. Antoniou, P.A. Nicolaou, A.A. De La Cruz, D.D. Dionysiou, Detoxification of water contaminated with the cyanotoxin, microcystin-LR, by utilizing thin TiO_2 photocatalytic films, in: *International Conference on Xenobiotics in the Urban Water Cycle*, Cyprus, 2009.
- [14] A. Aguadech, S. Brosillon, J. Morvan, L. El Kbir, *J. Hazard. Mater.* 150 (2008) 250.
- [15] A. Alatrache, N.A. Laoufi, M.N. Pons, J. Van Deik, O. Zahraa, *Water Sci. Technol.* 62 (2010) 434.
- [16] B. Mounir, M.N. Pons, O. Zahraa, A. Yaacoubi, A. Benhammou, *J. Hazard. Mater.* 148 (2007) 513.
- [17] G. Vincent, O. Zahraa, P.M. Marquaire, *J. Photochem. Photobiol., A* 197 (2008) 177.
- [18] M. Mezcuca, M.J. Gomez, I. Ferrer, A. Aguera, M.D. Hernando, A.R. Fernandez-Alba, *Anal. Chim. Acta* 524 (2004) 241.
- [19] G. Marci, V. Augugliaro, M.J.L. Munoz, C. Martin, L. Palmisano, V. Rives, M. Schiavello, R.J.D. Tilley, A.M. Venezia, *J. Phys. Chem. B* 105 (2001) 1033.
- [20] N. Barka, S. Qourzal, A. Assabbane, A. Nounah, Y. Ait-Ichou, *J. Photochem. Photobiol., A* 195 (2008) 346.
- [21] C. Guillard, J. Disidier, J.M. Herrmann, C. Lehaut, T. Chopin, S. Malato, *J. Blanco, Catal. Today* 54 (1999) 217.
- [22] G. Scacchi, M. Bouchy, J.-F. Foucaut, O. Zahraa, *Cinétique et catalyse, Tec& Doc, Lavoisier, Paris*, 1996.
- [23] D.D. Dionysiou, M.T. Suidan, I. Baudin, J.M. Lainé, *Appl. Catal., B* 38 (2002) 1.
- [24] A. Alatrache, A. Cortyl, P. Arnoux, M.N. Pons, O. Zahraa, *Toxicol. Environ. Chem.* 97 (2015) 32.
- [25] O. Ben Said, M.S. Goñi-Urriza, M. El Bour, M. Dellali, P. Aissa, R. Duran, *J. Appl. Microbiol.* 104 (2008) 987.
- [26] M.G. Antoniou, J.A. Shoemaker, A.A. De La Cruz, *Toxicol. Environ. Chem.* 51 (2008) 1103.
- [27] L. Mansouri, L. Boussemli, A. Ghrabi, *Water Sci. Technol.* 55 (2007) 119.
- [28] D. Vione, J. Feitosa-Felizzola, C. Minero, S. Chiron, *Water Res.* 43 (2009) 1959.
- [29] S. Thomas, A. Alatrache, M.N. Pons, O. Zahraa, *C. R. Chimie* 17 (2014) 824.